

Improvement of Dynamic Performance of Induction Motor Drives by using FLC Based MPFC

Sundilla Ravi, D. Krishna

Abstract: *This project proposes a model predictive flux control (MPFC) system based SVM for IM drive supplied by a three-level - neutral-point -clamped (3L-NPC) inverter with fuzzy logic controller. MPFC is a sort of effective control strategy for high operation of IM drives, which manages one of a kind momentary powerful reaction. be that as it may, MPFC experiences dull and time extreme alignment work for the weighting components, which is an obstacle for its utility, especially in the staggered converters. To fathom this inconvenience, it proposes MPFC machine principally dependent on SVM for IM drive. by methods for interpreting references of torque and stator motion size into an equivalent new stator motion vector reference, MPFC disposes of the utilization for weighting components. Fundamentally based at the FLC the pristine stator transition vector is the transpose to a voltage vector reference. that is then incorporated by means of a SVM square. The power of the proposed controller is confirmed by method for utilizing Matlab/Simulink in expressions nation and dynamic reactions.*

Index Choice: *Induction motor drive, MPFC, SVM, Fuzzy logic controller and Matlab/Simulink.*

I. INTRODUCTION

Model predictive flux control (MPFC) is featured with firm incentive response and simple structure. It is high power utilizations because of its lower voltage stress across semiconductor devices and less harmonic distortion in ac side. The 3L-NPC inverter is a standout among the maximum generally utilized staggered topologies in extensive electricity aircon drives. The 3L - NPC inverter - advocated IM drives have modified a legitimate research factor inside the scholarly community over the preceding many years [1], [2]. n currently, MPC has been provided as a hig execution manage conspire inside the area of depth converter and engine drives and is pulling in huge attention at some point of the arena [3]. however, MPC plans are inalienably computationally de-manding as a fundamental streamlining problem essentially to be settled. but, as cause for current be delineated, the organized control technique requires a system exertion that is exceedingly dwindled concerning be request feasible especially as a result of greater drives operating in the power unit district, mainly a lessening of the changing recurrence quick makes an interpretation of in to diminished misfortunes and, ultimately into vitality and fee reserve price range (regarding remember and established order) which might be superb in excessive have an effect on programs. This

manipulate method transporter some essential focal points. Offering additional manage destinations (like the equalization of the changing power misfortunes) is precise ahead. As all calculation are accomplished on the net, completely amounts is probably time fluctuated which include precedent parameters, orchestrate focuses, and physical marvel limits. Drastically extra vitally the controller may be right away linked to a prime class of three - stage air con power. some explicitly, enlistment machines (each squirrel - confine and ring - rotor type), synchronous and changeless - fascination machines can be tended to, and in addition inverter topologies, for instance, two, 3, 5 - stage inverters. but, to confound the clarification of the new control technique, we consciousness in this paper on a selected utility, where a NPC (three - level) voltage source inverter drives a squirrel - confine attractiveness engine [4]. Be that as it can, the control structure is mind boggling because of FL controller, SVM squares, and pivot change which moreover requires a high - desires shaft - established velocity engine. also, the vigor of the controller has noteworthy parameter reliance [5].sadly, with the amount of control elements expanding, all the greater weighting variables are required. especially the weighting additives of transition mistake λf and the coefficient variables of nonpartisan factor voltage λcv . but, it's miles dreary and tedious to tuning these weighting elements. To clean these issues. MPFC for two - stage inverter-advocated IM drives [6]. on this method, the quantity of stator transition and the examine of torque are modified over into another stator movement vector. The weighting variables of the transition errors λf can be stayed far from. there may be as yet a coefficient elements for NP voltage while making use of MPFC to 3 - degree electrical converter - nourished IM drives. To wipe out the weighting factors totally, a MPFC framework depending on SVM for a 3L - NPC electrical converter - endorsed IM drive is arranged on this paper. The similar stator motion vector which is changed over from the greatness of stator transition and torque [7], is changed into a stator voltage vector reference depending on the guideline of movement miscreant control, at that point the voltage vector is integrated by means of 3 - degree SVM dependent on bearer - primarily based PWM with zero grouping segment [8]. in this paper, to evacuate the stupid tuning paintings, the weighting elements is allotted with by using examining the relationship among torque and stator movement.

Revised Manuscript Received on December 28, 2018.

Sundilla Ravi, M. Tech Student, Anurag Group of Institutions, Hyderabad, Telangana, India

D. Krishna, Assistant Professor, Anurag Group of Institutions, Hyderabad, Telangana, India



In mild of the scientific case of IM, the references of torque and greatness of stator movement applied in convectional MPFC are identically changed over into any other reference vector of the stator movement. A value work comprising of following blunder of stator transition vector is then characterized and applied because the model to choose the first-class voltage vector. As simply the blunder of flux vector is evaluated in the new demand function, the weighting factor required in convectional MPFC is avoided in the planned method [7]. By distributing the duty cycle of redundant little voltage vectors dynamically, the NP potential fluctuation is limited in a small range. Hence, the weighting factor of NP voltage λ_{cv} can also be avoided

II. EQUATION OF DYNAMICIM

The stator flux ψ_s and stator current is as state variables, the energetic equations of IM in fixed reference frame as [9].

$$\frac{d}{dt} = Ax + Bu \quad (1)$$

$$\frac{di_s}{dt} = A_{11}i_s + A_{12}\psi_s + B_1u_s \quad (2)$$

$$\frac{D\psi_s}{dt} = A_{21}i_s + u_s \quad (3)$$

Where $x = [i_s \ \psi_s]^T$ are state variables ; $u = u_s$ is the state voltage vector and

$$A_{11} = -\lambda(R_s L_r + R_r L_s) + j\omega_r \quad (4)$$

$$A_{12} = \lambda(R_r - jL_r\omega_r) \quad (5)$$

$$A_{21} = -R_s \quad (6)$$

$$B_1 = \lambda L_r \quad (7)$$

Where R_s, R_r, L_s, L_r and L_m are the stator resistance, rotor resistance, stator inductance, rotor inductance and mutual inductance , respectively; ω_r is the rotor speed and $\lambda = \frac{1}{(L_s L_r - L_m^2)}$. Equation (2) must be discretized to predict flux and torque (k+1)th instant for a given voltage vector. A simple way to discretize (2) is using first order Euler method. An improved discrete model of IM is obtained by using the Cayley – Hamilton theorem to compute, the matrix exponential, which is quite complicated. To achieve higher accuracy and avoid complicated calculation, the Heun's method [10] is employed in this paper which is expressed as

$$i_s^{k+1} = i_{sp}^k + (A_{11}i_s^k + A_{12}\psi_s^k + B_1u_s^k) t_{sc} \quad (8)$$

$$\psi_{sp}^{k+1} = \psi_s^k + (A_{21}i_s^k + u_s^k) t_{sc} \quad (9)$$

$$i_s^{k+1} = i_{sp}^{k+1} + \frac{t_{sc}}{2} (A_{11}(i_{sp}^{k+1} - i_s^k) + A_{12}(\psi_{sp}^{k+1} - \psi_s^k)) \quad (10)$$

$$\psi_s^{k+1} = \psi_{sp}^{k+1} + \frac{t_{sc}}{2} (A_{21}(i_{sp}^{k+1} - i_s^k)) \quad (11)$$

Where t_{sc} is control period, i_s^{k+1} and ψ_{sp}^{k+1} are predictor-corrector i_s^{k+1} and ψ_s^{k+1} are predicted stator current and stator flux at (k+1)th instant respectively.

The rotor flux at (k+1)th instant can be estimated from stator flux ψ_s^{k+1} and current i_s^{k+1} as

$$\psi_r^{k+1} = \frac{L_r}{L_m} \psi_s^{k+1} - \frac{1}{\lambda L_m} i_s^{k+1} \quad (12) \text{ and } \text{the}$$

electromagnetic torque can be predicted as [1]:

$$T_s^{k+1} = \frac{3}{2} N_p \lambda L_m (\psi_r^{k+1} \otimes \psi_s^{k+1}) \quad (13)$$

Where N_p is the number of pole pairs and \otimes speaks to move produced using vectors? The circuit of acceptance motor drive encouraged by utilizing a 3L NPC inverter is appeared in figure.1. The inverter produces three explicit scopes of voltage on the output terminal by interfacing the yield shaft to the fabulous transport barp, Negative transport bar n or nonpartisan point o on this paper different levels are named as 2, zero ,1 individually. As demonstrated in figure2, the inverter produces 27 voltage vectors in four categories; Big voltage vectors (BVV), Medium voltage vectors (MVV), Small voltage vectors (SVV) and Zero voltage vectors (ZVV).It should be noted that there are a pair of SV Vs producing the equal line voltage, but their consequences on nonpartisan point voltage are inverse the impartial point voltage stability is mainly achieved via editing the responsibility cycle of inverse SV Vs during one control period. The deviation of the nonpartisan factor voltage is defined as the distinction between the top capacitor voltage and the decrease capacitor voltage within the dc interface.

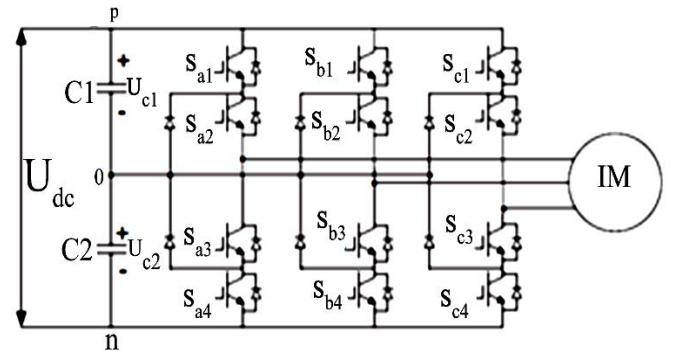


Fig. 1. Circuit topology of induction motor drive fed by a 3L NPC inverter

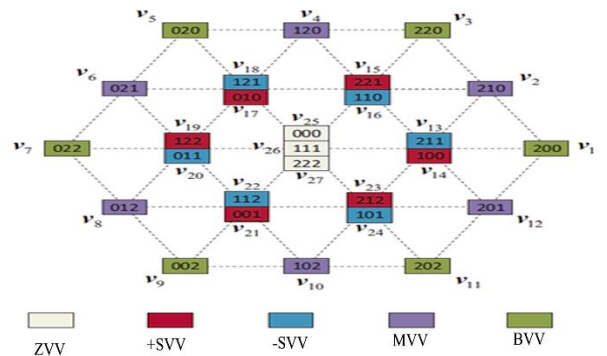


Fig. 2. Space vector graph of 3L NPC inverter

$$\Delta U_{mid} = U_{c1} - U_{c2} \quad (14)$$

III. PRINCIPLE OF THE PROPOSED MPFC

The control diagram of the proposed MPFC is shown in fig 2, that is particularly made out of the accompanying parts: finish arrange onlooker, put off repayment, reference transformation, dead beat oversee of stator flux, three – degree SVM. The torque order is gotten by means of an outside speed control circle the use of FLC. The stator transition adequacy is kept predictable because of the reality the motion – debilitate activity isn't contemplated in this paper. The focused on coming of alternate components inside the oversee chart might be expounded inside the accompanying printed content.

A. Full Order Observer

To obtain the information of stator flux a closed loop full request onlooker is embraced in this paper. This sort of spectator can accomplish great precision over a wide speed go and has some strength against machine parameter varieties. The mathematical model of the observer is expressed [1]

$$\frac{dx}{dx} = A\hat{x} + Bu_s + G(i_s - \hat{i}_s) \quad (15)$$

Where $\hat{x} = [\hat{i}_s \hat{\psi}_s]^T$ are state variables representing the estimated stator current and stator flux. A constant gain matrix G is employed to improve stability of the observer which is expressed as

$$G = \begin{bmatrix} 2b \\ b \end{bmatrix} \quad (16)$$

Where b is a negative constant gain [1]. This gain matrix is very effective and simple to implement. In digital implementation, the observer is discretized using Heun's method introduced in Section II. More details regarding this observer can be found in [1].

After obtaining the estimated stator current and stator flux at k^{th} instant from (5), the rotor flux can be estimated as

$$\hat{\psi}_r = \frac{L_r}{L_m} \hat{\psi}_s - \frac{1}{\lambda L_m} \hat{i}_s \quad (17)$$

B. Reference Conversion and Delay Compensation

In this section, a new stator flux vector reference ψ_s^{ref} is equivalently constructed from T_e^{ref} and ψ_r^{ref} based on the interval relationship of IM. The magnitude of stator flux vector reference ψ_s^{ref} is set to the rated value ψ^{ref} when the machine runs below the rated speed, namely that:

$$|\psi_s^{ref}| = \psi^{ref} \quad (18)$$

The torque can be expressed as a cross product of stator flux and rotor flux, which is shown as (4). Meanwhile, the rotor flux ψ_r is estimated by (3). According to (4), the references of T_e^{ref} and ψ_r^{ref} exists a equation as following:

$$\psi_s^{ref} = \psi_s^{ref} \exp(j \angle \psi_s^{ref}) \quad (19)$$

$$\angle \psi_s^{ref} = \angle \psi_r + \arcsin\left(\frac{T_e^{ref}}{\frac{3}{2} N_p \lambda L_m |\psi_r| \psi_r^{ref}}\right)$$

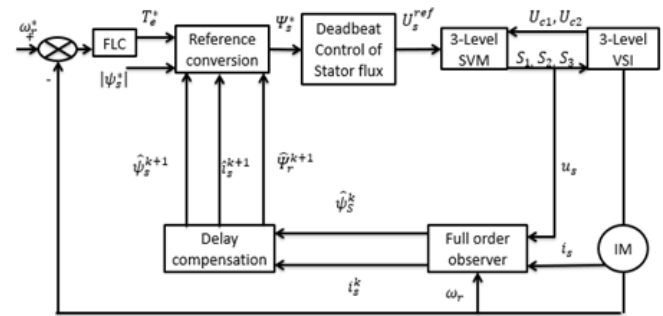


Fig.3. Control diagram of the three – vectors – based MPFC

Based on (13), (19), and (20), the new stator flux vector reference ψ_s^{ref} is transferred from the reference T_e^{ref} and ψ_r^{ref} .

In digital implementation, there is usually one step delay among decided on voltage vectors and implemented voltage vectors to compensate this put off, the stator flux vector reference ψ_s^{ref} at $(k+1)$ th instant should be predicted. Hence the cost function is expressed as [1].

$$J_1 = |\psi_s^{ref} - \psi_s^{k+2}| \quad (21)$$

At the same time the rotor flux at $(k+2)$ th instant can be predicted from:

$$\psi_r^{k+2} = \psi_r^{k+1} + T_{sc} [R_r \frac{L_m}{L_r} i_s^{k+1} (\frac{R_r}{L_r} - j\omega_r^{k+1}) \psi_r^{k+1}] \quad (22)$$

As the sampling interval is much smaller than the mechanical time-constant of the rotor [4], the rotor speed ω_r is assumed to be constant, $\omega_r^{k+1} = \omega_r^k$.

The phase angle of ψ_s^{ref} at $(k+2)$ th instant can be computed from torque reference T_e^{ref} and predicted rotor flux ψ_r^{k+2} as:

$$\angle \psi_s^{ref} = \angle \psi_r^{k+2} + \arcsin\left(\frac{T_e^{ref}}{\frac{3}{2} N_p \lambda L_m |\psi_r^{k+2}| \psi_r^{ref}}\right) \quad (23)$$

Where ψ_s^{k+1} and i_s^{k+1} are computed from (2).

C. Deadbeat Control of Stator Flux Based on SVM

Knowing the stator flux amplitude ψ^{ref} and its angle from (10), the next step is to achieve deadbeat control of stator flux. From (1), the stator voltage vector reference in stationary frame can be obtained as

$$U_s^{ref} = R_s i_s^{k+1} + \frac{\psi_s^{ref} - \psi_s^{k+1}}{T_{sc}} \quad (24)$$

For 3L – NPC inverter, voltages across two capacitors should be balanced. Large capacitor voltage unbalance may harm the semiconductor devices and prompts the torque and transition swells [3].

By method for the utilization of SVM, this issue can be effectively fathomed. The stator voltage vector joined statesref is

Orchestrated the use of SVM of the three exchanging state vectors which are closest to the reference vector at each inspecting prompt. At that point, the SVM methodology creates 12 PWM signals for the switches of 3L – NPC inverter. The SVM system is actualized dependent on administration basically based PWM with zero – grouping component [11], [14].

In many occasions, there are as a base several [SVV] _s alluded to as fantastic SVV and awful SVV in an oversee length [15]. As eminent [SVV] _S and poor [SVV] _S are indistinguishable in significance and area however connected to unique transport bar, they are indistinguishable from the engine aspect yet opposite for fair point Voltage control [16]. By utilizing changing the general span of at that point, impartial point voltage blunder might be redressed. If one SVV is beneficial to neutral point voltage balance, namely $\Delta U_{mid} \rightarrow 0$, its duty cycle should be extended while the other's shortened. The adjustive ratio can be either a constant or a time – variant value. It should be noted that a larger adjustive ratio leads to better neutral point voltage balance but more narrow pulses.

D. Fuzzy Logic Controller

The most significant variables entering the fuzzy logiccontroller has been selected as the error and its time variation. The output of the FLC is the variation of command current. The two inputs variables e and $ce(k)$, are calculated at every sampling instant as one output:

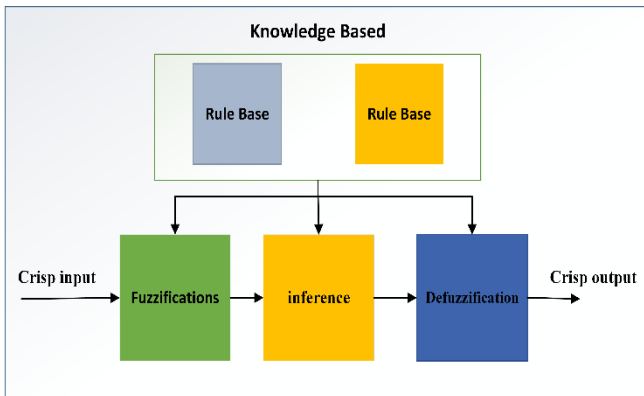


Fig. 4. Fuzzy logic controller internal structure

$$e\omega(k) = \omega_r^*(k) - \omega_r(k) \quad (25) \quad ce\omega(k) = e\omega(k) - e\omega(k-1) \quad (26)$$

where $\omega_r^*(k)$ is the reference speed and $\omega_r(k)$ is the actual rotor speed. As shown in Fig. 4. The FLC consists of three stages: fuzzification, rule execution, and defuzzification.

In the first stage, the crisp variables $e\omega(k)$ and $ce\omega(k)$ are converted into fuzzy variables $e\omega$ and $ce\omega$. Membership functions associated to the control variables have been chosen with triangular shapes as shown in Fig. 4. The universes of discourse of the input variables $e\omega$ and $ce\omega$ are established after many simulations as $(-1, 1)$ rad/s and $(-1, 1)$ rad/s,

respectively. The universe of discourse of the output variable ci_{qs}^* is $(-1.5, 1.5)$ A. Each universe of discourse is divided in to seven fuzzy sets: NB (Negative Big), NM (Negative Medium), NS (Negative Small), ZE (Zero), PS (Positive Big), PM (Positive Medium), PS (Positive Small). Each fuzzy variable is a member of the subsets with a degree of membership μ varying between 0 (non-member) and 1 (full member). Moreover, in other to get a good sensitivity, a better thickness of subsets has been worked close to the 0 estimation of the manage factors. In the 2nd phase of the FLC, the factors $e\omega$ and $ce\omega$ are dealt with by way of a deduction motor that executes 49 rules (7x7) as appeared inside the Tab. 1. Those standards are built up using the information of the framework enrolment and the revel in of the manage engineers. Every well-known is communicated in the form as in the accompanying version: IF ($e\omega$ is Negative Medium) AND ($ce\omega$ is Positive Small) THEN (ci_{qs}^* is Negative Small). Different inference methods can be used to produce the fuzzy set values for the output fuzzy variable ci_{qs}^* . In this paper, the Max-Product inference method [2] is used to calculate the final fuzzy value ci_{qs}^* of the output.

In the defuzzification stage, a crisp value of the output variable $ci_{qs}^*(k)$ is obtained by using the tallness defuzzification method, wherein the centroid of each yield enrolment work for each standard is first assessed. The specific last yield is then determined on the grounds that the normal of the individual centroids, weighted through their statures (degree of membership) as follow:

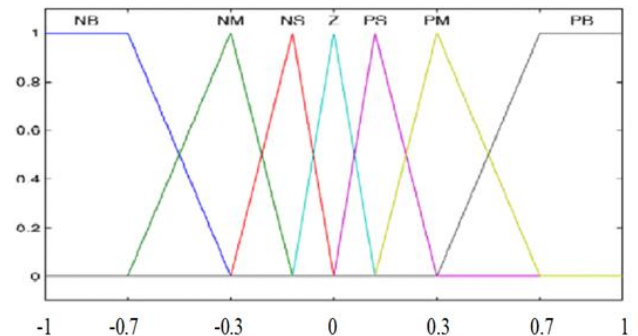


Fig. 5. Membership function for input 1ce.

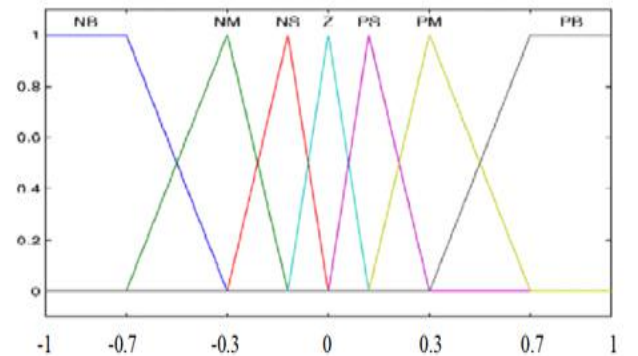


Fig. 6. Membership function for input 2, ce.

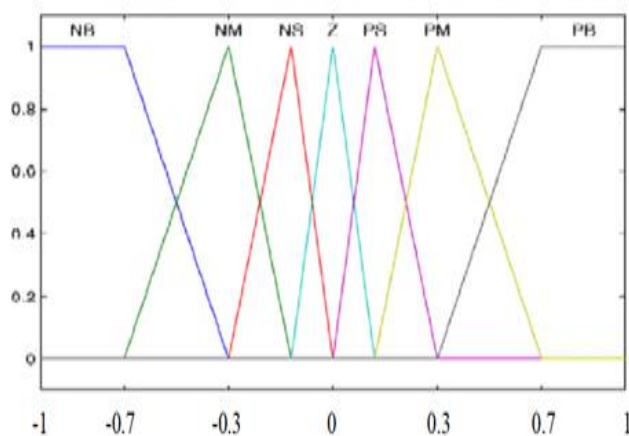


Fig.7. Membership function of output c_{qs}^*

$$c_{qs}^*(k) = \frac{\sum_{i=1}^n \mu[(c_{qs}^*)_i] (c_{qs}^*)_i}{\sum_{i=1}^n \mu[(c_{qs}^*)_i]} \quad (27)$$

The reference current $i_{qs}^*(k)$ that is applied to the vector control system is computed by integrating $c_{qs}^*(k)$:

$$i_{qs}^*(k) = i_{qs}^*(k-1) + c_{qs}^*(k) \quad (28)$$

Error \ Fuzzy Output	NB	NM	NS	ZE	PS	PM	PB
NB	NB	NB	NB	NB	NM	NS	ZE
NM	NB	NB	NB	NM	NS	ZE	PS
NS	NB	NB	NM	NS	ZE	PS	PM
ZE	NB	NM	NS	ZE	PS	PM	PB
PS	NM	NS	ZE	PS	PM	PB	PB
PM	NS	ZE	PS	PM	PB	PB	PB
PB	ZE	PS	PM	PB	PB	PB	PB

Table.1. Rule Table

IV SIMULATION RESULTS

Fig.13.shows the speed and torque characteristics of conventionalPI and FLC. It appears that the rise time decreases when fuzzy controller is added to simulation model and both results are taken in same period of time. Fig.14.shows It is observed that when the event of introductory transient, with fuzzy controller the engine settles at 1.9466 Sec even as in case of PI it is 1.8787 Sec. Fig.15. demonstrates the torque and speed response for step alternate in the heap torque utilising the PI and fuzzy controller. Engine begins from halt at load torque of 100 Nm at $t = 0.6$ Sec and a unexpected complete heap of seven-hundred Nm is connected to the framework. for that reason, the time taken by way of the PIcontroller to perform unfaltering kingdom is a lot better than fuzzy controller.

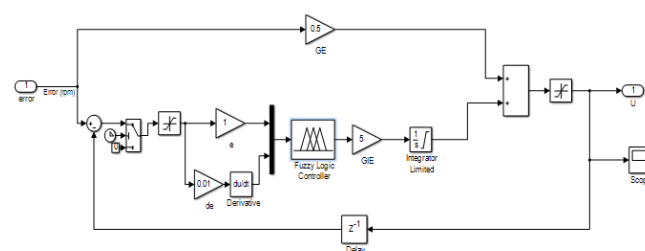


Fig. 9. Simulink diagram of fuzzy logic controller

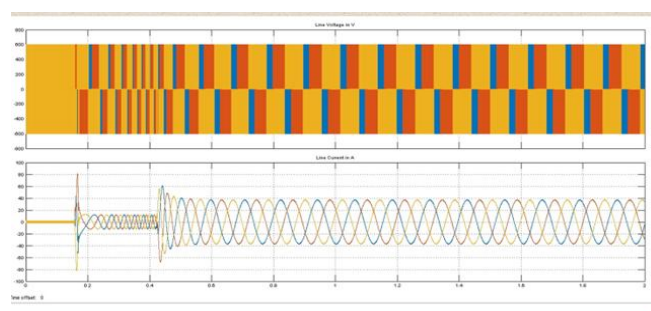


Fig. 10. Voltage and current waveforms of PI controller

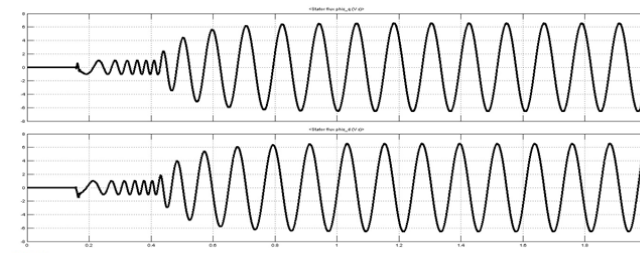


Fig. 11. d-q stator flux of PI controller

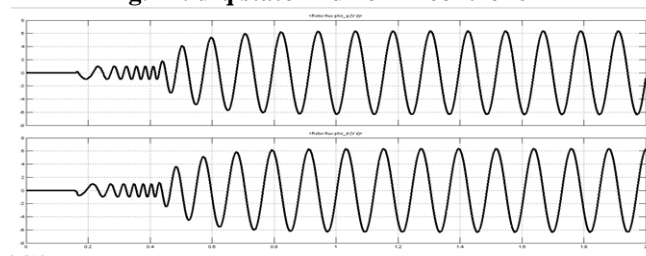


Fig. 12. d-q rotor flux of PI controller

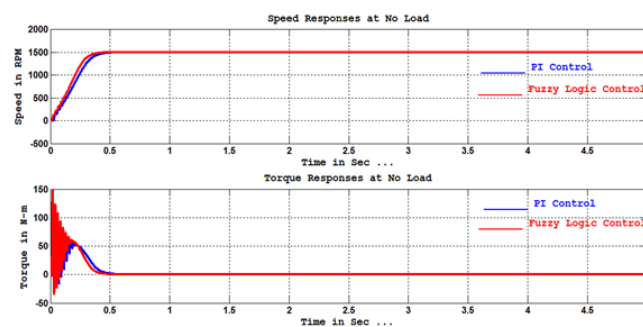


Fig. 13. TorqueSpeed characteristics of PI and Fuzzy controller at no load

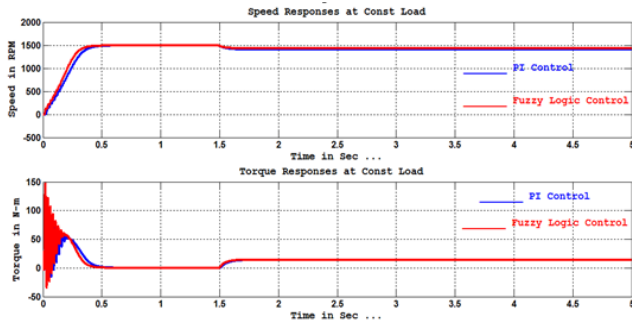


Fig. 14. TorqueSpeed characteristics of PI and Fuzzy controller at constant Load

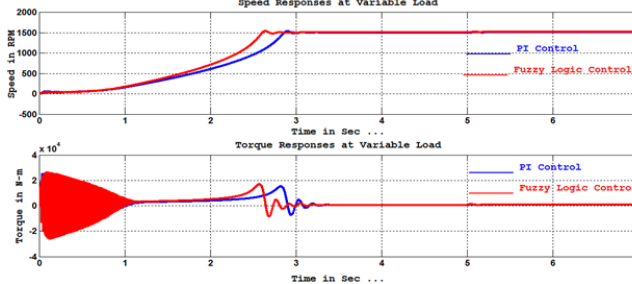


Fig. 15. TorqueSpeed characteristics of PI and Fuzzy controller at variable Load

V. CONCLUSION

This paper proposes a MPFC system based on SVM for IM drive supplied by a 3L-NPC inverter. The reference voltage vector exchanged from control factors is combined by SVM. with the guide of changing the relative commitment cycles of SVVs, the proposed strategy smoothes the nonpartisan factor voltage variation within the torque and speed reaction for step trade in the load torque the utilization of the PI and fluffy controller. Engine starts from stop at load torque of a hundred Nm at $t = 0.6$ Sec and a astonishing complete heap of 700 Nm is done to the system. consequently, the time taken with the guide of the PI controller to increase steady state is tons superior to fluffy controller of the dc-hyperlink voltage at predictable kingdom. Moreover, decoupled control of stator flux and torque are finished under stand-out working circumstances. Fitting consistent state exhibitions and brisk dynamic responses are done on a similar time. as contrasted and conventional MPFC, complex weighting components tuning is eliminated completely. Recreation results are introduced to confirm the effectiveness of the proposed plans.

REFERENCES

1. Y. Zhang, J. Zhu, Z. Zhao, W. Xu, and D. G. Dorrell, "An improved direct torque control for three-level inverter-fed induction motor sensorless drive," *IEEE transactions on power electronics*, vol. 27, no. 3, pp. 1502–1513, 2012.
2. Y. Zhang and Y. Peng, "Performance evaluation of direct power control and model predictive control for three-level ac/dc converters," in *Energy Conversion Congress and Exposition (ECCE)*, 2015 IEEE, IEEE, 2015, pp. 217–224.
3. Y. Zhang, B. Xia, and H. Yang, "Performance evaluation of an improved model predictive control with field-oriented control as a benchmark," *IET Electric Power Applications*, vol. 11, no. 5, pp. 677–687, 2017.

4. T. Geyer, G. Papafotiou, and M. Morari, "Model predictive direct torque control—part i: Concept, algorithm, and analysis," *IEEE Transactions on Industrial Electronics*, vol. 56, no. 6, pp. 1894–1905, 2009.
5. M. Habibullah, D. D.-C. Lu, D. Xiao, and M. F. Rahman, "Finite-state predictive torque control of induction motor supplied from a three-level npc voltage source inverter," *IEEE Transactions on Power Electronics*, vol. 32, no. 1, pp. 479–489, 2017.
6. Y. Zhang, H. Yang, and B. Xia, "Model-predictive control of induction motor drives: Torque control versus flux control," *IEEE Transactions on Industry Applications*, vol. 52, no. 5, pp. 4050–4060, 2016.
7. Y. Zhang and H. Yang, "Two-vector-based model predictive torque control without weighting factors for induction motor drives," *IEEE Transactions on Power Electronics*, vol. 31, no. 2, pp. 1381–1390, 2016.
8. F. Wang, "Sine-triangle versus space-vector modulation for three-level pwm voltage-source inverters," *IEEE transactions on industry applications*, vol. 38, no. 2, pp. 500–506, 2002.
9. J. Holtz, "The representation of ac machine dynamics by complex signal flow graphs," *IEEE Transactions on Industrial Electronics*, vol. 42, no. 3, pp. 263–271, 1995.
10. S. C. Chapra and R. P. Canale, *Numerical methods for engineers*. McGraw-hill New York, 1998, vol. 2.
11. Z. Keliang and W. Danwei, "Relationship between space-vector modulation and three-phase carrier-based pwm: A comprehensive analysis [three-phase inverters]," *Industrial Electronics, IEEE Transactions on*, vol. 49, no. 1, pp. 186–196, 2002.
12. N. Celanovic and D. Boroyevich, "A comprehensive study of neutral-point voltage balancing problem in three-level neutral-point-clamped voltage source pwm inverters," *IEEE Transactions on power electronics*, vol. 15, no. 2, pp. 242–249, 2000.
13. J. H. Seo, C. H. Choi, and D. S. Hyun, "A new simplified space-vector pwm method for three-level inverters," *IEEE Transactions on power electronics*, vol. 16, no. 4, pp. 545–550, 2001.
14. B. K. Bose, "Expert system, fuzzy logic, and neural network applications in power electronics and motion control," *Proceedings of the IEEE*, vol. 82, no. 8, pp. 1303–1323, 1994.